Bulgarian Chemical Communications, Volume 57, Issue 4 (pp. 259-266) 2025 *DOI: 10.34049/bcc.57.4.5644*

Role of chemicals in dye-sensitized solar cells based on liquid-phase electrolyte for generation of electrical energy

A. Susawat[1], D. Meena[1], G. Meena[1], R.K. Meena[1], L. Baloat[1], Disha[2], A.S. Meena[1*]

[1]*Department of Chemistry, University of Rajasthan, Jaipur, Rajasthan-302004, India*
[2] *Department of Applied Science and Humanities, BK Birla Institute of Engineering and Technology, Pilani, Rajasthan-333031, India*

Received: May 03, 2024; Revised: September 11, 2025

The present study investigates the role of chemicals, such as methyl orange, in combination with fructose and sodium lauryl sulfate, in dye-sensitized solar cells (DSSCs) based on liquid-phase electrolyte for solar energy conversion. The liquid-phase electrolyte-based DSSC operates by converting solar energy into electrical energy through the formation of energy-rich intermediates that exhibit photogalvanic effect. The measured photovoltaic parameters of the cell include an open-circuit potential of 1090.0 mV and a short-circuit current of 670.0 μA. The conversion efficiency and fill factor are calculated to be 4.68% and 0.2603, respectively. The storage capacity of the cell, evaluated in dark conditions, is determined to be 225.0 min. In addition, the influence of various parameters on the electrical output is examined, and the current-voltage (J-V) characteristics are analyzed. A possible mechanism for photocurrent generation in the electrolyte-based dye-sensitized solar cell is also proposed.

Keywords: photogalvanic effect, potential, current, conversion efficiency, storage capacity

INTRODUCTION

A large, affordable, and sustainable source of energy is essential for the progress of developing nations. Among the available non-conventional resources, solar energy represents the most abundant and freely accessible renewable option. The growing demand for renewable energy technologies has intensified the interest in liquid-phase electrolyte-based dye-sensitized solar cells (DSSCs) owing to their potential for efficient solar energy conversion and storage. These systems operate by converting solar energy into electrical energy through the formation of energy-rich intermediates that exhibit photogalvanic effect. This phenomenon was first identified by Rideal and Williams and was later systematically investigated by Rabinowitch [2, 3], followed by several other researchers. Over the years, extensive efforts have been devoted to improving the performance and efficiency of liquid-phase electrolyte-based dye-sensitized solar cells [4-8]. Research in this field has explored the use of various photosensitizers, mixed sensitizers with reductants, and electrolyte systems incorporating surfactants to enhance solar energy conversion and storage [9-15]. Recently, Meena and co-workers have developed liquid-phase electrolyte-based solar cells utilizing diverse photosensitizer-reductant combinations for electrical energy generation [16-18]. Building upon these advancements, the present study focuses on investigating the role of chemical constituents in a liquid-phase electrolyte-based dye-sensitized solar cell employing chemicals such as methyl orange as photosensitive compound along with fructose as the reductant, and sodium lauryl sulfate as the surfactant.

Materials and methodology

Methyl orange (Merck), sodium lauryl sulfate (Loba Chemie), fructose (Merck), and NaOH (Merck) were employed in this study. All solutions were prepared using doubly distilled water. Stock solutions were obtained by direct weighing of the reagents and stored in light-protected containers.

The dye-sensitized solar cell (DSSC) based on a liquid-phase electrolyte was systematically assembled for photovoltaic studies [19-21]. The system consists of an electrochemically treated platinum foil as the working electrode and a saturated calomel electrode (SCE) as the reference electrode. The distance between illuminated and dark electrodes was maintained at 45 mm. Illumination was provided by a 200 W tungsten lamp, with a water filter used to eliminate infrared radiation. The photopotential was measured as the difference between the initial potential of the cell in the dark and the equilibrium potential attained under continuous illumination. Initially, the potential was recorded in the dark, and changes in potential upon illumination were monitored as a function of time.
Prior to experimentation, the solutions were purged

* To whom all correspondence should be sent:
E-mail: *anoopsingh10786@gmail.com*

with purified nitrogen gas for approximately 20 min to remove dissolved oxygen.

The experimental solution, containing the dye, reductant, surfactant, and NaOH, was placed in an H-type glass cell. A platinum electrode (1.0 × 1.0 cm^2) was immersed in one arm of the H-tube, while the SCE was positioned in the other. The system was first stabilized in the dark, after which the platinum electrode arm was illuminated with the tungsten lamp, while the SCE arm was kept in the dark. The photochemical bleaching of methyl orange was monitored potentiometrically. A digital pH meter (Systronics Model-335) and a microammeter (Ruttonsha Simpson) were employed to measure the photopotential and photocurrent, respectively.

The current-voltage (J-V) characteristics of the solar cell were determined by applying an external load through a carbon potentiometer (log 470 K), connected in the circuit *via* a key to allow both open- and closed-circuit measurements. The overall experimental setup of the electrolyte-based dye-sensitized solar cell is shown in Figure 1. Furthermore, the influence of various parameters on the performance of the cell was systematically investigated [22-24]. The rate of potential decay after removal of illumination was determined to be 3.30 mV min^{-1}.

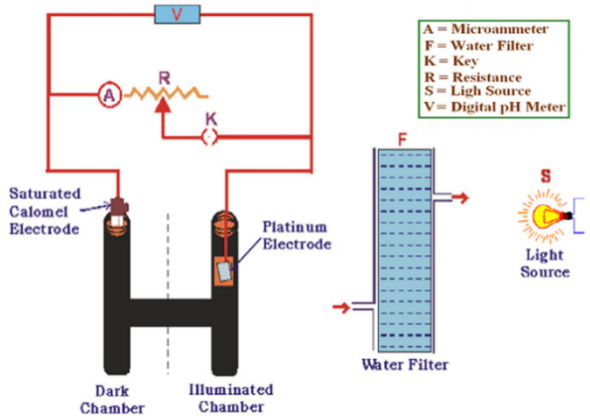

Figure 1. Experimental set-up of dye-sensitized solar cell (based on liquid phase electrolyte)

RESULTS AND DISCUSSION

Structure and absorption spectrum of the photosensitive compound (methyl orange)

Methyl orange (MO), chemically known as dimethylaminoazobenzene sulfonate, is a commonly used anionic azo dye. It is a water-soluble compound primarily applied as a pH indicator. Due to its widespread use in the textile, paper, printing, and food industries, substantial quantities of methyl orange are released into industrial wastewater. Its distinct color variation with pH makes it particularly valuable in acid-base titrations. In acidic medium, methyl orange appears red, while in basic medium it exhibits a yellow coloration. This property makes it suitable for titrations involving moderately strong acids, as its transition occurs near the pKa value. The molecular structure and UV-visible absorption spectrum of methyl orange (λ_{max} = 464 nm) are presented in Figure 2.

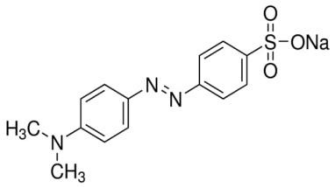

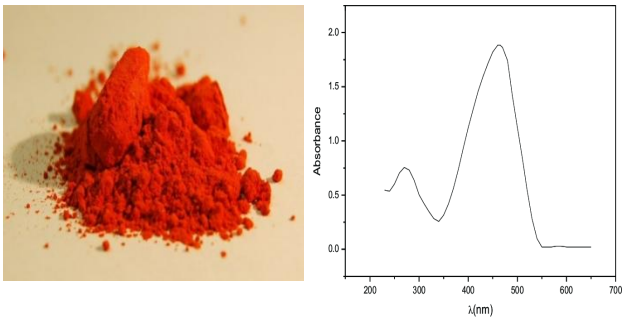

Figure 2. Structure and UV-vis spectrum of the photosensitive compound (methyl orange)

Variation of photovoltaic parameters with time

The photopotential of the dye-sensitized solar cell (DSSC) based on a liquid-phase electrolyte was measured at different pH values, with the maximum value observed at pH 12.70. Consequently, all subsequent experiments were carried out at this pH value. The variation of photopotential with time is shown in Figure 3(A). Upon illumination, the photopotential steadily increases and reaches 1090.0 mV within approximately 100.0 min, after which it remains constant despite continued illumination. When the light source is switched off, the system does not return to its initial potential, indicating incomplete reversibility.

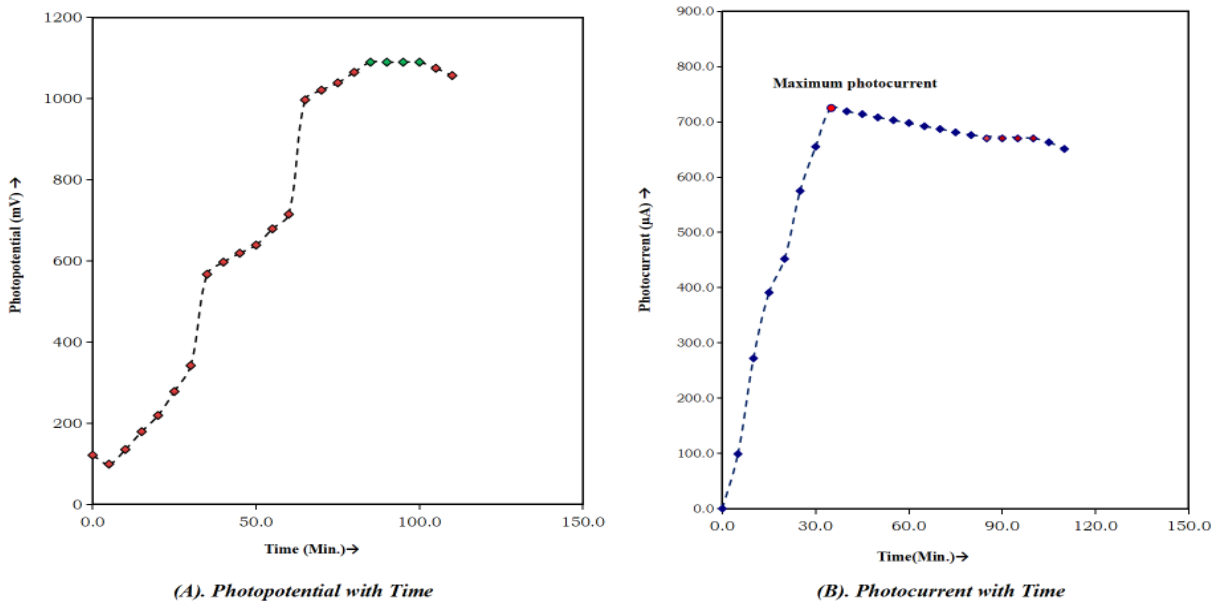

Figure 3. Variation of photovoltaic parameters with time

The photocurrent shows a rapid increase upon illumination and attains its maximum value, denoted as I_{max}, within a few min. The short-circuit photocurrent of the DSSC containing the liquid electrolyte composed of methyl orange, fructose, and sodium lauryl sulfate is presented in Figure 3(B). Under illumination, the equilibrium photocurrent reaches 670.0 μA after 100.0 min for the cell containing the specific concentration ratio of the electrolyte components [23, 25].

Effect of electrolyte concentration on cell's photovoltaic parameters

The optimum cell performance is observed at a concentration of 2.28×10^{-5} M for the photosensitive compound, methyl orange (Figure 4A). At concentrations below this value, the electrical output decreases due to the limited number of photosensitive molecules available to absorb light and donate electrons to the platinum electrode. At concentrations above 2.28×10^{-5} M, excess photosensitive molecules prevent sufficient light from reaching the molecules near the electrode surface, resulting in a corresponding decrease in the cell's power output.

The optimum cell performance is observed at a concentration of 1.62×10^{-3} M for the reducing agent, fructose (Figure 4B). At lower concentrations, fewer fructose molecules are available to donate electrons to the photosensitive molecules, which reduces the electrical output. At higher concentrations, the increased presence of fructose promotes back electron transfer from the photosensitive molecules to fructose and hinders the motion of photosensitive molecules toward the electrode, thereby causing a decline in cell power.

The role of micellar species is essential in enhancing the solubility of photosensitive molecules in dye-sensitized solar cells based on liquid-phase electrolytes. The photo-ejection of electrons from excited photosensitive molecules depends on the charge properties of surface-active agents such as sodium lauryl sulfate (SLS). These surfactant molecules facilitate the separation of photo-products through hydrophilic–hydrophobic interactions, thereby improving the conversion efficiency and storage capacity of the liquid-phase electrolyte in the dye-sensitized solar cell [26-28].

The optimum cell performance is observed at a concentration of 1.29×10^{-3} M for the surface-active compound, sodium lauryl sulfate (Figure 4C). The variation in electrical output arises because micelles solubilize photosensitive molecules to the greatest extent at or near their critical micelle concentration (CMC). Below this concentration, fewer photosensitive molecules dissolve in the electrolyte solution, leading to reduced electrical output. At concentrations above 1.29×10^{-3} M, excess surfactant prevents the proper dissolution of photosensitive molecules, as higher concentrations promote the formation of other aggregates such as lamellar structures and rod-like micelles in solution, as well as analogous bilayers and multilayers at interfaces, thereby causing a corresponding decrease in cell power [29-31].

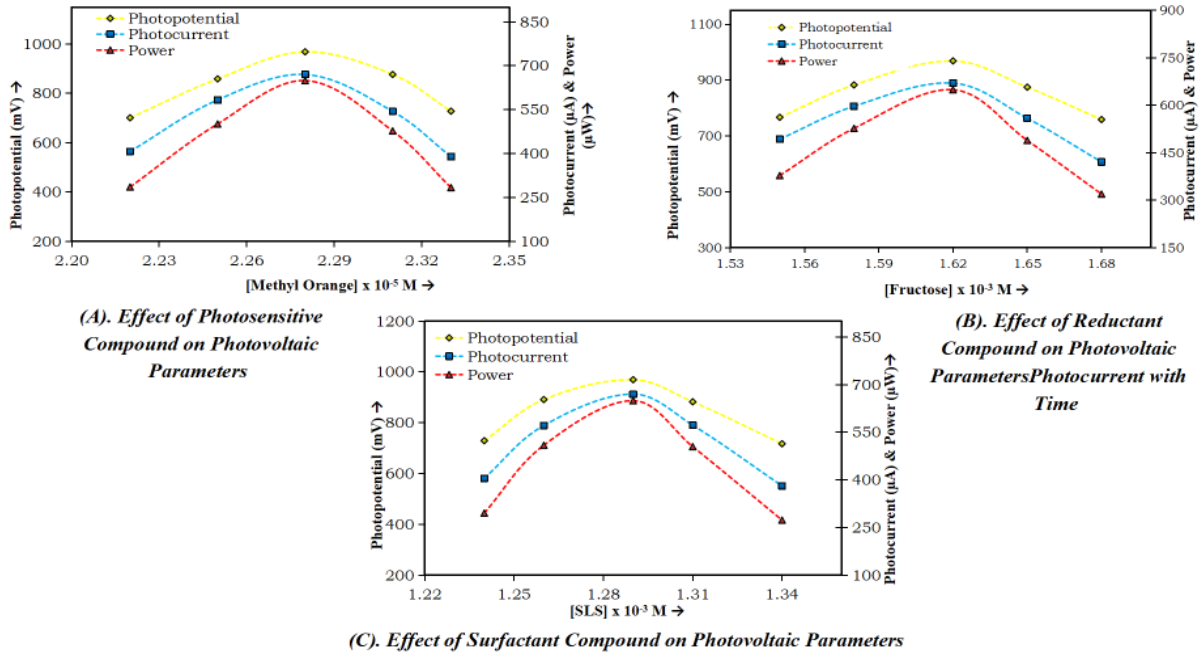

Figure 4. Effect of electrolyte concentration on cell's photovoltaic parameters

Table 1. Effect of pH of electrolyte solution on cell's photovoltaic parameters

[Methyl orange] = 2.28 × 10^{-5} M [NaLS] = 1.29 × 10^{-3} M [Fructose] =1.62 × 10^{-3} M	Light intensity = 10.4 mW cm^{-2} Temperature = 303 K				
	pH				
Liquid phase electrolyte DSSCsl	12.62	12.66	12.70	12.74	12.78
Photopotential (mV)	727.0	873.0	969.0	859.0	709.0
Photocurrent (μA)	359.0	562.0	670.0	538.0	317.0
Power (μW)	260.99	490.63	649.23	462.14	224.75

Table 2. Effect of (A) Diffusion length and (B) Electrode area on cell's photovoltaic parameters

[Methyl orange] = 2.28 × 10^{-5} M [NaLS] = 1.29 × 10^{-3} M [Fructose] = 1.62 × 10^{-3} M	Light intensity = 10.4 mW cm^{-2} pH = 12.70 Temperature = 303 K				
(A) Diffusion length (mm)					
Diffusion length (mm)	35.0	40.0	45.0	50.0	55.0
Maximum photocurrent Imax (μA)	707.0	716.0	725.0	733.0	741.0
Equilibrium photocurrent Ieq (μA)	688.0	679.0	670.0	661.0	652.0
Rate of photocurrent (μA min^{-1})	20.20	20.46	20.71	20.94	21.17
(B) Electrode area (cm^2)					
Electrode area (cm^2)	0.70	0.85	1.00	1.15	1.30
Maximum photocurrent Imax (μA)	711.0	717.0	725.0	734.0	742.0
Equilibrium photocurrent Ieq (μA)	685.0	677.0	670.0	662.0	653.0

Effect of pH of electrolyte solution on cell's photovoltaic parameters

A liquid-phase electrolyte-based dye-sensitized solar cell (DSSC) exhibits pronounced sensitivity to the pH of the electrolyte solution. An increase in pH within the alkaline range results in a corresponding enhancement of the photovoltaic parameters, namely potential and current, with maximum values recorded at pH 12.70. Beyond this point, further increases in pH cause a decline in electrical output.

The optimum pH condition was found to correlate with the pKa of the reductant, where the effective range occurred at pH > pKa. This behavior is attributed to the greater availability of the reductant molecules in their anionic form, which act as more efficient electron donors within the electrolyte solution. The corresponding results are summarized in Table 1.

Effect of diffusion length and area of electrode on cell's photovoltaic parameters

The influence of diffusion length, defined as the distance between the two electrodes, on the photoelectric parameters of the DSS cell, namely maximum photocurrent (Imax), equilibrium photocurrent (Ieq), and initial rate of photocurrent generation was investigated using a H-type cell based on liquid-phase electrolyte of varying dimensions. The effect of electrode area on these parameters was also examined. Results indicated that both Imax and initial rate of photocurrent generation ($\mu A \cdot min^{-1}$) increase with diffusion length, whereas Ieq shows a slight decrease. This variation in electrical output was attributed to the involvement of electroactive species, specifically the leuco or semi-leuco forms of the dye (photosensitizer) in the illuminated and dark chambers, respectively. The reductant molecules and their oxidation products serve exclusively as electron carriers within the electrolyte solution of the dye-sensitized solar cell. The dependence of the photoelectric parameters on the diffusion length is summarized in Table 2A, while Table 2B presents the variation with electrode area. Furthermore, it is observed that Imax increases with electrode area, whereas Ieq correspondingly decreases.

$$\textit{Fill Factor (FF)} = \frac{Vpp \times Ipp}{Voc \times Isc}$$

Current-voltage (J-V) characteristics of the dye-sensitized solar cell

The short-circuit current (*Isc*) and open-circuit voltage (*Voc*) of the cell were measured under closed- and open-circuit conditions using a digital pH meter and a multimeter, respectively [32-35]. Intermediate current and potential values between these two limits were obtained by applying an external load through a carbon potentiometer (log 470 K) connected to the multimeter circuit. The current-voltage (J-V) characteristics of the dye-sensitized solar cell are summarized in Table 3 and illustrated graphically in Figure 5.

Table 3. Current-voltage (J-V) characteristics of the DSS cell

Liquid phase electrolyte based DSS cell	*Voc* (mV)	*Isc* (μA)	*Vpp* (mV)	*Ipp* (μA)	*FF*
	1090.0	670.0	555.0	340.0	0.2584

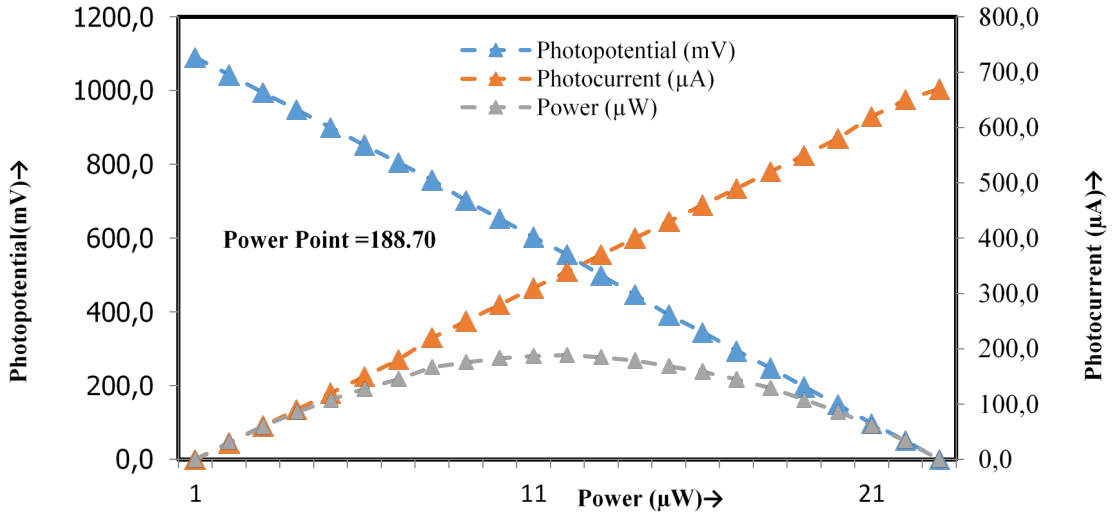

Figure 5. Current-voltage (J-V) characteristics of the cell.

Performance of the dye-sensitized solar cell

The performance of the dye-sensitized solar cell based on a liquid-phase electrolyte is evaluated by applying an external load after the light source is switched off, once the potential stabilizes (to achieve current at the power point, represented by red and green color symbols in Figure 5). The output power is assessed in terms of $t_{1/2}$, defined as the time required for the power to decay to 50% of its maximum value under dark conditions [36-38]. Experimental results demonstrate that the cell operates in complete darkness for up to 225 minutes. The corresponding data are summarized in Table 4 and are graphically presented in Figure 6.

Table 4. Performance of the dye-sensitized solar cell based on liquid phase electrolyte

Liquid phase electrolyte based DSS cell	Charging time (min)	Power (μW)	Power at $t_{1/2}$ (μW)	$t_{1/2}$ (min)
	100.0	188.70	95.01	225.0

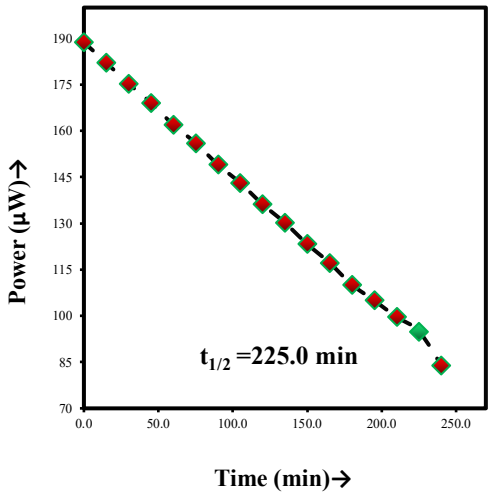

Figure 6. Performance of the dye-sensitized solar cell based on liquid phase electrolyte

Conversion efficiency of the cell [39-41]

The conversion efficiency of the cell was calculated from the photocurrent and photopotential values at the power point, together with the incident radiation power, and was found to be 4.68% (Table 5).

$$\text{Conversion efficiency}(\%) = \frac{V_{pp} \times i_{pp}}{10.4 mW cm^{-2} \times Electrode\ area\left(cm^2\right)} \times 100$$

Table 5. Conversion efficiency of the dye-sensitized solar cell based on liquid phase electrolyte

Liquid phase electrolyte based DSS cell	FF	CE (%)	Storage capacity (%)
	0.2584	4.68	2.25 %

Mechanism

On the basis of these observations, the following mechanism is proposed for photocurrent generation in the liquid phase electrolyte-based dye-sensitized solar cell [42-44] (Fig. 7).

CONCLUSION

At present, the world is experiencing a severe energy crisis, and meeting the increasing energy demand remains a significant challenge for all nations. This situation necessitates the development of renewable energy devices capable of generating electrical energy for extended durations. In the present study, this issue is addressed through the utilization of a liquid-phase electrolyte containing suitable components in a dye-sensitized solar cell (DSSC), yielding promising results. The photovoltaic performance is investigated using an electrolyte composed of methyl orange as photosensitizer, fructose as reductant, and sodium lauryl sulfate as surfactant, with particular emphasis on the effects of pH, diffusion length, and electrode area. Based on the findings, it is concluded that an efficient liquid-phase electrolyte-based DSSC can be fabricated, exhibiting appreciable conversion efficiency and notable energy storage capacity [45-47].

Acknowledgement: *The authors sincerely acknowledge the Head, Department of Chemistry, University of Rajasthan, Jaipur (Rajasthan-302004, India), for providing the necessary laboratory facilities to conduct this research. One of the authors (A.S. Meena) gratefully acknowledges the University Grants Commission (UGC), Government of India, New Delhi, for the financial assistance provided to this work.*

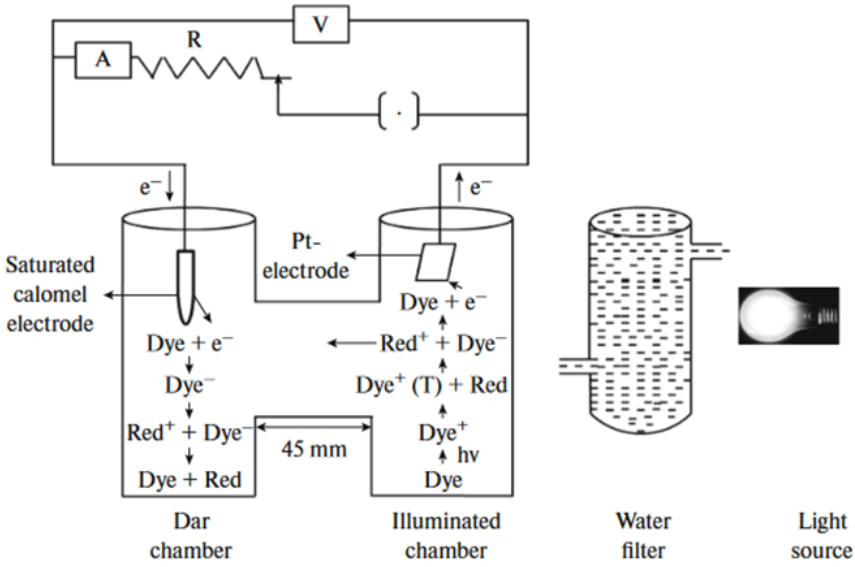

Figure 7. Mechanism of dye-sensitized solar cell based on liquid phase electrolyte

REFERENCES

1. E.K. Rideal, E.G. Williams, *Journal of the Chemical Society Transactions*, **127**, 258 (1925).
2. E. Rabinowitch, *The Journal of Chemical Physics*, **8**(7), 551 (1940).
3. E. Rabinowitch, *The Journal of Chemical Physics*, **8**(7), 560 (1940).
4. A.E. Potter Jr, L.H. Thaller, *Solar Energy*, **3**(4), 1 (1959).
5. K.M. Gangotri, C. Lal, *Proceedings of the Institution of Mechanical Engineers, Part A: Journal of Power and Energy*, **219**(5), 315 (2005).
6. S. Madhwani, J. Vardia, P.B. Punjabi, V.K. Sharma, *Proceedings of the Institution of Mechanical Engineers, Part A: Journal of Power and Energy*, **221**(1), 33 (2007).
7. S.C. Ameta, P.B. Punjabi, J. Vardia, S. Madhwani, S. Chaudhary, *Journal of Power Sources*, **159**(1), 747 (2006).
8. K.K. Rohatgi-Mukherjee, M. Bagchi, B.B. Bhowmik, *Electrochimica Acta*, **28**(3), 293 (1983).
9. C. Lal, *Journal of Power Sources*, **164**(2), 926(2007).
10. K.R. Genwa, M. Genwa, *Solar Energy Materials and Solar Cells*, **92**(5), 522 (2008).
11. K.R. Genwa, N.C. Khatri, *Energy & Fuels*, **23**(2), 1024 (2009).
12. P. Gangotri, P. Koli, *Sustainable Energy & Fuels*, **1**(4), 882 (2017).
13. S. Yadav, R.D. Yadav, G. Singh, *Int. J. Chem. Sci*, **6**(4), 1960 (2008).
14. A. Malviya, P.P. Solanki, *Renewable and Sustainable Energy Reviews*, **59**, 662 (2016).
15. K.M. Gangotri, M.K. Bhimwal, *International Journal of Energy Research*, **35**(6), 545 (2011).
16. M. Chandra, R.C. Meena, *Research Journal of Chemical Sciences,* **1**, 1 (2011).
17. A.S. Meena, P.L. Meena, M. Chandra, R.C. Meena, *International Journal of Renewable Energy Research*, **3**(2), 276 (2013).
18. S.L. Meena, R.K. Bhupesh, L.C. Yadav, *Journal of Applied Science and Education (JASE)*, **3**(1), 1 (2023).
19. J. Rathore, A. Rakesh Kumar, P. Sharma, M. Lal, *Indian J. Sci. Technol.*, **15**(23), 1159 (2022).
20. Z. Li, S. Wang, J. Wu, W. Zhou, *Renewable and Sustainable Energy Reviews*, **156**, 111980 (2022).
21. S.R. Saini, S.L. Meena, R.C. Meena, *Advances in Chemical Engineering and Science*, **7**(2), 125 (2017).
22. W. Peng, M.Z. Shaik, C. Pascal, C. Raphael, R. Humphry-Baker, M. Gratzel, *J. Phys. Chem. B,* **107**, 14336 (2003).
23. M. Azzouzi, T. Kirchartz, J. Nelson, *Trends in Chemistry*, **1**(1), 49 (2019).
24. X. Liu, X. Du, J. Wang, C. Duan, X. Tang, T. Heumueller, G. Liu, Y. Li, Z. Wang, J. Wang, F. Liu, *Advanced Energy Materials*, **8**(26), 1801699 (2018).
25. S. Liu, J. Yuan, W. Deng, M. Luo, Y. Xie, Q. Liang, Y. Zou, Z. He, H. Wu, Y. Cao, *Nature Photonics*, **14**(5), 300 (2020).
26. H. Yao, Y. Cui, D. Qian, C.S. Ponseca Jr, A. Honarfar, Y. Xu, J. Xin, Z. Chen, L. Hong, B. Gao, R. Yu, *Journal of the American Chemical Society*, **141**(19), 7743 (2019).
27. F.D. Eisner, M. Azzouzi, Z. Fei, X. Hou, T.D. Anthopoulos, T.J.S. Dennis, M. Heeney, J. Nelson, *Journal of the American Chemical Society*, **141**(15), 6362 (2019).
28. E.T. Efaz, M.M. Rhaman, S. Al Imam, K.L. Bashar, F. Kabir, M.E. Mourtaza, S.N. Sakib, F.A. Mozahid, *Engineering Research Express*, **3**(3), 032001 (2021).
29. S.R. Fatemi Shariat Panahi, A. Abbasi, V. Ghods, M. Amirahmadi, *Journal of Materials Science: Materials in Electronics*, **31**(14), 11527 (2020).

30. A.S. Meena, L. Baloat, S.C. Meena, D. Meena, *Int. J. Creative Research Thoughts (IJCRT)*, **12**(8), 29 (2024).
31. A.S. Meena, Jayshree, L. Baloat, *Int. J. Creative Research Thoughts (IJCRT)*, **10**(7), 315 (2022).
32. A.M. Adeyinka, O.V. Mbelu, Y.B. Adediji, D.I. Yahya, *Int. J. Energy Power Eng.,* **17**(1), 1 (2023).
33. A.S. Meena, Sonika, *Int. J. Res. & Anal. Reviews (IJRAR),* **9**(2), 454 (2022).
34. K. ElKhamisy, H. Abdelhamid, E.S.M. El-Rabaie, N. Abdel-Salam, *Plasmonics*, **19**(1), 1 (2024).
35. M.K. Bhimwal, K.M. Gangotri, A. Pareek, J. Kumar, *Int. J. Innovative Research in Technology*, **9**(3), 632 (2022).
36. M. Zghaibeh, P.C. Okonkwo, W. Emori, T. Ahmed, A.M.A. Mohamed, M. Aliyu, G.J. Ogunleye, *International Journal of Green Energy*, **20**(5), 555 (2023).
37. A.S. Meena, Jayshree, Sonika, D. Meena, *J. Emerging Tech.& Innovative Research (JETIR),* **9**(6), 825 (2022).
38. S. Wijewardane, L.L. Kazmerski, *Solar Compass*, **7**, 100053 (2023).
39. A.S. Meena, *J. Modern Chemistry and Chemical Tech.,* **12**(1), 20 (2021).
40. G. Regmi, A. Ashok, P. Chawla, P. Semalti, S. Velumani, S.N. Sharma, H. Castaneda, *Journal of Materials Science: Materials in Electronics*, **31**(10), 7286 (2020).
41. A.S. Meena, Sonika, Jayshree, M. Akram, H. Posawl, M.L. Meena, J. Meena, *Asian J. Chemical & Envi. Res.,* **14**(1-4), 30 (2021).
42. S. Sivaraj, R. Rathanasamy, G.V. Kaliyannan, H. Panchal, A. Jawad Alrubaie, M. Musa Jaber, Z. Said, S. Memon, *Energies*, **15**(22), 8688 (2022).
43. M.G. Buonomenna, *Symmetry*, **15**(9), 1718 (2023).
44. N.S. Seroka, R. Taziwa, L. Khotseng, *Materials*, **15**(15), 5338 (2022).
45. R. Dallaev, T. Pisarenko, N. Papež, V. Holcman, *Materials*, **16**(17), 5839 (2023).
46. A. Maalouf, T. Okoroafor, Z. Jehl, V. Babu, S. Resalati, *Renewable and Sustainable Energy Reviews*, **186**, 113652 (2023).
47. S.M. Sivasankar, C.D.O. Amorim, A.F.D. Cunha, *Journal of Composites Science*, **9**(3), 143 (2025).